4

Electrochemical CO_2 reduction to formic acid on a Pd-based formic acid oxidation catalyst

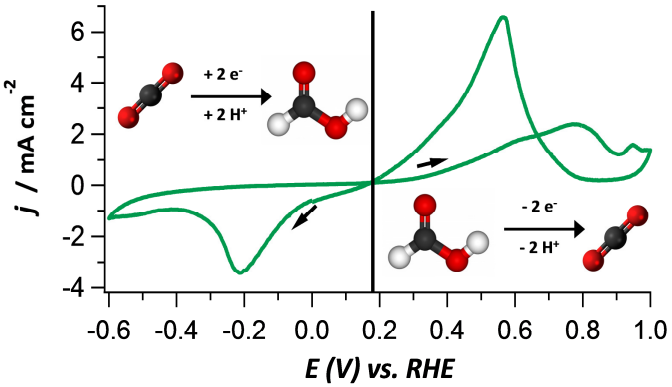

The contents of this chapter have been published as: R. Kortlever, C. Balemans, Y. Kwon and M.T.M. Koper, *Catal. Today* **2015**, *244*, 58-62.

Abstract The electrochemical reduction of CO_2 is a reaction of much current interest as a possible reaction for energy storage. In this Chapter, we show that on electrodeposited palladium on platinum, a good formic acid oxidation catalyst, the onset potential for CO_2 reduction to formic acid is dramatically reduced in comparison to bulk palladium. Two different reaction pathways are observed; a pathway at low overpotential in which formic acid is produced from either direct bicarbonate reduction or from the reduction of CO_2 generated from bicarbonate near the surface, and a pathway at more negative potentials where formic acid is produced from direct CO_2 reduction. Furthermore, we show that reversible formic acid oxidation and CO_2 reduction is possible on this catalyst, although unfortunately the processes are hindered by poisoning of the catalyst, most likely by CO.

4.1 Introduction

The electrochemical reduction of CO_2 has attracted much attention in the last decades, since it is a potential process for energy storage and production of synthetic fuels.[1,2] When coupled to renewable energy sources, the utilization of CO_2 by electroreduction to fuels could not only have the advantage of replacing fossil fuel-based energy sources, but also lowering CO_2 emissions into the atmosphere. However, at the moment the main problems that inhibit electrochemical CO_2 reduction from being applied are the high overpotentials and the poor product selectivity.[3] Therefore, a key challenge in present research is the development of catalysts that efficiently and selectively reduce CO_2 to useful products.

One of these useful products is formic acid, since it can be used directly as a building block for fine chemicals and as a fuel in direct formic acid fuel cells (DFAFCs).[4,5] Formate and formic acid are the main products in CO_2 reduction on poor metals, such as Pb, Hg, Tl, In, Sn, Cd and Bi. Unfortunately, these materials are generally not very useful for applications since they require very negative potentials (≈ -2.0 V vs. SCE) to achieve good selectivities.[3,6] Some recent efforts have decreased the overpotentials needed to produce formic acid on these catalysts, but the overpotentials are still significant.[7]

In biological systems, formate dehydrogenase enzymes show efficient reduction of CO_2 to formic acid at low overpotentials. Armstrong and Hirst have recently discussed how these redox enzymes can reversibly catalyze reaction 1:[8]

$$HCOOH \leftrightarrows CO_2 + 2\,H^+ + 2\,e^- \qquad (1)$$

but there is no fundamental reason why inorganic metallic catalysts could not do the same, since "reversible electrocatalysts" are expected to exist for two-electron transfer reactions.[9] Metallic catalysts that are very active for formic acid oxidation are mostly palladium- or platinum-based catalysts.[5,10] These materials experience some difficulties however in the electrochemical reduction of CO_2. Platinum, for instance, reduces CO_2 to adsorbed CO, which then blocks the platinum surface.[3,11] Moreover, both palladium and platinum are very good catalysts for the hydrogen evolution reaction (HER), which occurs as a side reaction simultaneously with CO_2 reduction and thus lowers the faradaic efficiency towards useful products made from CO_2. Interestingly, Sánchez-Sánchez et. al recently reported that by modifying platinum single crystal electrodes with adsorbed adatoms the activity of the electrodes towards CO_2 reduction can be enhanced.[12]

In this Chapter we report the formulation of a palladium-based catalyst system that is able to produce formic acid from CO_2 with a low overpotential. This catalyst is based on the idea that for a two-electron transfer reaction, such as reaction 1, reversible catalysts must exist; this implies that catalysts that are very active for the electrochemical oxidation of formic acid should also be active for the reverse electrochemical reduction of CO_2 to formic acid. Therefore, our catalyst is not only able to reduce CO_2 at low potentials but is also able to oxidize formic acid, thus showing reversible catalytic behaviour.

4.2 Experimental

4.2.1 Electrochemical measurements

All electrochemical experiments were carried out in an electrochemical cell using a three-electrode assembly at room temperature. The cell and all other glassware were first cleaned by boiling in a 1:1 mixture of concentrated sulfuric and nitric acid and were cleaned before every experiment by boiling in ultra-pure water (Millipore MilliQ gradient A10 system, 18.2 MΩ cm). A coiled gold wire was used as counter electrode. All potentials are reported versus the reversible hydrogen electrode (RHE) as reference electrode in a separate compartment filled with the same electrolyte, at the same pH as the electrolyte in the electrochemical cell.

Cylindrical polycrystalline platinum and palladium electrodes (99.9% Pd and 99.99% Pt, purchased at Mateck GmbH) with a diameter of 5 mm embedded in teflon were used as working electrode. Prior to every experiment the working electrode was polished mechanically to a mirrorlike finish using alumina pastes. After this, the electrode was sonicated in ultra-pure water. Cyclic voltammograms at a scan rate of 50 mV s^{-1} were recorded on an Ivium A06075 potentiostat.

Electrolytes were made from ultra-pure water and high purity reagents (Merck Suprapur, Sigma Aldrich TraceSelect). Before each experiment electrolytes were first purged with Argon (Air Products, 5.7) for 15 minutes to remove air from the solution, after which they were purged with CO_2 (Linde, 4.5) for at least 30 minutes to saturate the solutions.

4.2.2 OLEMS

Online Electrochemical Mass Spectrometry (OLEMS) was used to detect gaseous products of the reactions. The products were collected with a small hydrophobic tip which was positioned close (about 10 µm) to the electrode with the aid of a camera.[13] The tip was constructed as a porous Teflon cylinder with a diameter of 0.5 mm and an average pore size of 10-14 µm in a Kel-F holder. The tip is connected to a mass spectrometer with a PEEK capillary. Before use the tip was cleaned in a solution of 0.2 M $K_2Cr_2O_7$ in 2 M H_2SO_4 and rinsed thoroughly with Millipore water. A secondary electron multiplier (SEM) voltage of 2400 V was used

for detection in a Balzers Quadrupole mass spectrometer, except for hydrogen (m/z = 2) where a SEM voltage of 1200 V was used. The products were measured while changing the potential of the electrode from 0.0 V to -1.5 V, unless mentioned otherwise, and back at 1 mV s^{-1}.

4.2.3 Online HPLC

Products dissolved in the electrolyte were detected using online High Performance Liquid Chromatography (HPLC).[14] While changing the potential from 0.0 V to the required potential, samples were collected with an open tip positioned close (≈ 10 µm) to the electrode. Sampling was done at a rate of 60 µL min^{-1} and each sample had a volume of 60 µL. Since the potential was changed at 1 mV s^{-1}, each sample contained the products averaged over a potential change of 60 mV. After voltammetry, these samples were analyzed by HPLC (Prominence HPLC, Shimadzu; Aminex HPX 87-H column, Biorad).

4.3 Results and Discussion

4.3.1 CO_2 reduction on palladium and platinum

We first describe CO_2 reduction on unmodified palladium and platinum electrodes. Platinum shows no difference between a blank cyclic voltammogram with argon and a voltammogram with CO_2 in solution. However, this was not the case with palladium (see Figure 4.1). The cyclic voltammograms with CO_2 in solution show a decrease in reduction current compared to the blank voltammograms. This is an indication that palladium is active for the reduction of CO_2, as is already well known.[15,16] In accordance with earlier reports,[15,16] formic acid was observed as the dominant soluble product at very negative potentials.

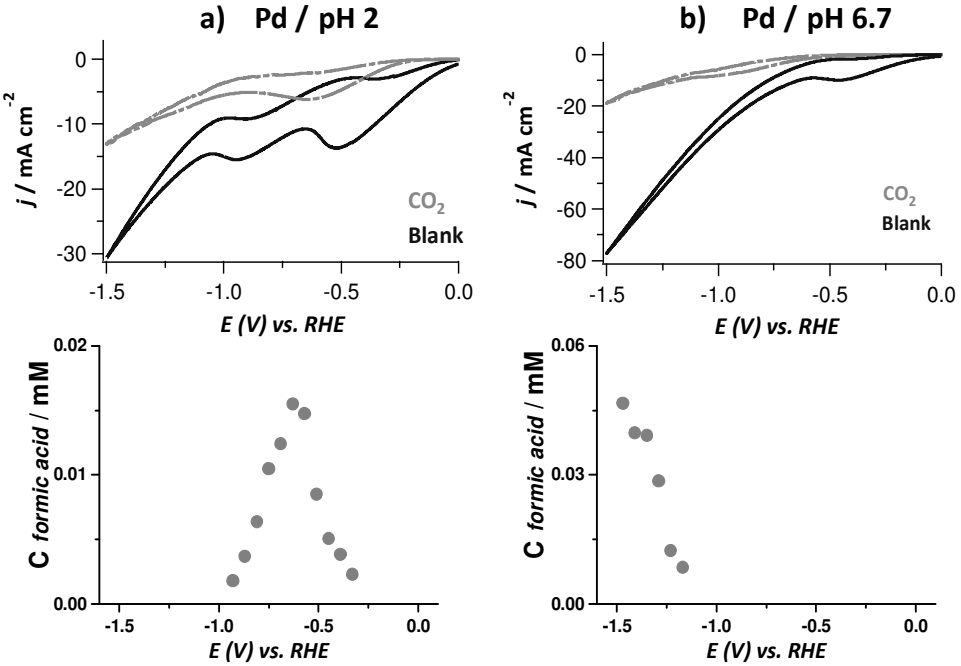

Figure 4.1 a) Cyclic voltammograms of a palladium electrode in a phosphate buffer at pH 6.7 (0.1 M H_3PO_4/ 0.1 M KH_2PO_4) at a scan rate of 50 mV/s in the presence of CO_2 (grey dash) and in the presence of argon (black) and formation of formic acid detected with online HPLC using a phosphate buffer at pH 2 (0.1 M H_3PO_4/ 0.1 M KH_2PO_4) saturated with CO_2, **b)** Cyclic voltammograms of a palladium electrode in a phosphate buffer at pH 6.7 (0.1 M KH_2PO_4/ 0.1 M K_2HPO_4) at a scan rate of 50 mV/s in the presence of CO_2 (grey dash) and in the presence of argon (black) and formation of formic acid detected with online HPLC using a phosphate buffer at pH 6.7 (0.1 M KH_2PO_4/ 0.1 M K_2HPO_4).

Interestingly, the production of formic acid on a palladium electrode turns out to be very pH dependent since the onset potential for formic acid production on palladium at pH 6.7 is -1.2 V vs. RHE, while at pH 2 it is -0.35 V vs. RHE (see Figure 4.1). Furthermore, at pH 2 formic acid is only produced between –0.35 V and -0.95 V vs. RHE with a peak at -0.75 V vs. RHE, while at pH 6.7 formic acid production increases from -1.2 V vs. RHE to lower potentials. Hydrogen and traces of methane and ethylene were detected with OLEMS as gaseous products in a pH 6.7 electrolyte (> -1.2 V vs. RHE) (see Figure 4.2).

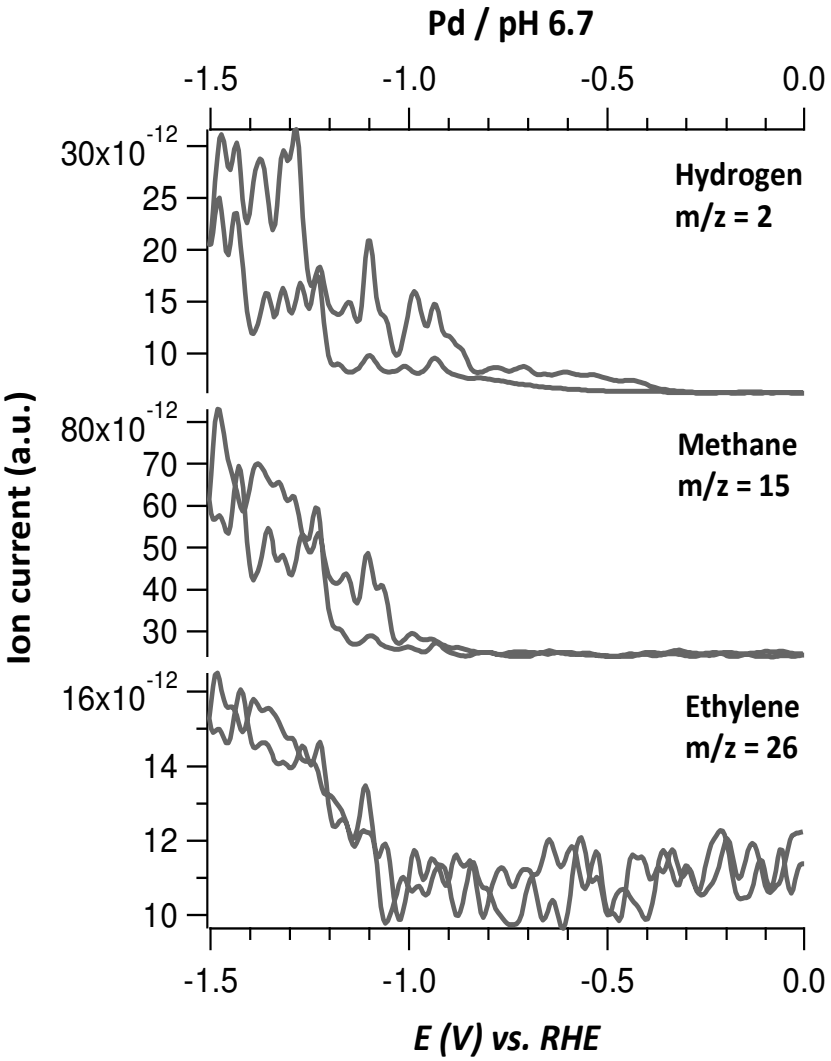

Figure 4.2 Formation of hydrogen (m/z = 2), methane (m/z = 15) and ethylene (m/z = 26) from CO_2 reduction on Pd followed with OLEMS; a) in a pH 2 posphate buffer electrolyte (0.1 M H_3PO_4/ 0.1 M KH_2PO_4), b) in a pH 6.7 phosphate buffer electrolyte (0.1 M KH_2PO_4/ 0.1 M K_2HPO_4).

4.3.2 Electrodeposition of palladium on a platinum substrate

Baldauf and Kolb showed that the deposition of palladium on a platinum electrode yields a surface that is highly active for formic acid oxidation.[17] To study this combination for CO_2 reduction, palladium was electrodeposited on a polycrystalline platinum electrode, using a modification of the deposition method of Baldauf and Kolb, by depositing palladium onto platinum from a 0.1 M H_2SO_4 + 0.1 mM $PdCl_2$ solution at +0.27 V vs. SCE for a period of 60s.

The structure of these layers was imaged with scanning electron microscopy (SEM) (see Figure 4.3), showing that palladium completely covers the platinum substrate. The palladium structures are mostly triangular shaped, suggesting a preferential (111) configuration. Some defects are observed, mostly holes in the deposition layer (black dots in the SEM images), but the concentration of these defects on the surface is low, so that we do not expect that these defects will play a major role in the catalytic properties of the material. The palladium layers show a roughened nanostructured surface, making it impossible to determine the exact thickness of the palladium overlayers on platinum, since this will vary along the electrode surface. However, from the coulombic charge of the palladium deposition, which was typically between 6-6,5 mC, an average palladium thickness of 65 – 75 monolayers of palladium was estimated. Copper UPD measurements showed that the surface area increased

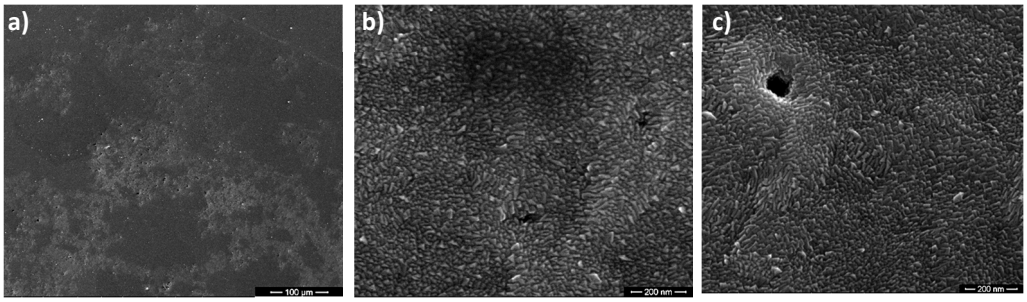

Figure 4.3 Scanning electron microscopy (SEM) images of palladium electrodeposited on platinum at +0.27 V vs. SCE for 60s at different length scales; a) scale of 100 µm, b) scale of 200 nm, c) scale of 200 nm and under a 20˚ angle.

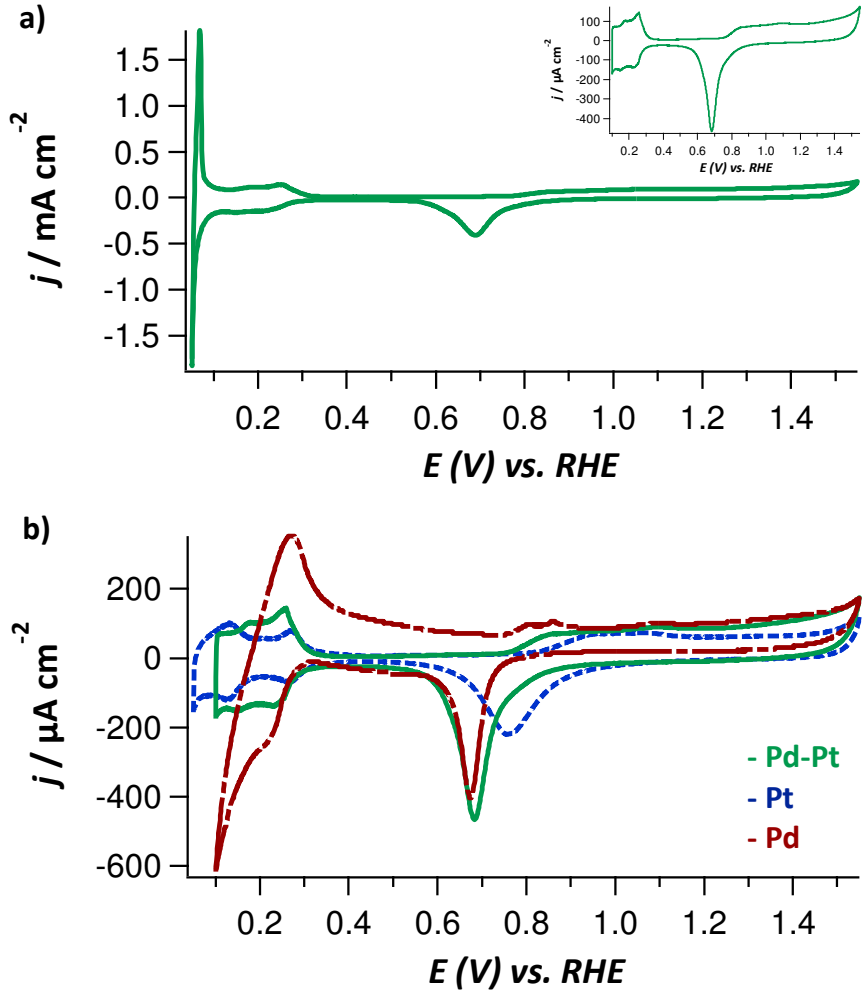

Figure 4.4 a) Cyclic voltammogram of a Pd-Pt electrode in a 0.5 M H_2SO_4 electrolyte starting at 0.05 V vs. RHE, inset starting at 0.1 V vs. RHE, both at a scan rate of 20 mV/s, b) comparison of voltammograms of Pd-Pt (green stripe), platinum (blue dots) and palladium (red dots and stripes) in a 0.5 M H_2SO_4 electrolyte at a scan rate of 20 mV/s.

1.15 times compared to the bare Pt electrode.

The Pd-Pt electrode was characterized by blank voltammetry in 0.5 M H_2SO_4 and compared with platinum and palladium (see Figure 4.4). In the voltammograms with Pd-Pt electrode very sharp peaks for hydrogen oxidation and hydrogen reduction are seen between 0.05 V and 0.1 V vs. RHE (Figure 4.4a). These peaks in the voltammetry have been seen before for Pd-Pt alloys with both palladium and platinum at the surface.[18] This would imply that before or during the voltammetry platinum has migrated towards the surface, thus partially covering the surface. The oxide formation and reduction peaks of the Pd-Pt electrode are similar to Pd, suggesting the existence of a Pd layer on the surface, whereas the absence of a hydrogen absorption current in the hydrogen region suggests that the Pd layer must be thin. Since the voltammograms are very similar to voltammograms seen for Pd-Pt alloys and since there is no hydrogen absorption current in the hydrogen region, we hypothesize that we have formed a surface alloy of palladium and platinum.

4.3.2 CO_2 reduction on a Pd-Pt electrode

Cyclic voltammograms of CO_2 reduction on the Pd-Pt electrode were recorded in a pH 6.7 phosphate buffer (see Figure 4.5). A clear decrease in current can be seen in the CO_2 reduction scan compared to a blank scan in an argon atmosphere (Figure 4.5a). This is an indication that the Pd-Pt electrode interacts with CO_2. Furthermore, a reduction peak between -0.1 V and -0.6 V vs. RHE is seen in the presence of CO_2 that is not seen in the blank scan (Figure 4.5b), which is likely due to CO_2 reduction. This peak is no longer observed in the second scan (Figure 4.5b) suggesting that a poison may have formed on the surface.

When the upper potential of the voltammogram is changed from 0 V vs. RHE to 1.0 V vs. RHE a stripping peak is seen around 0.8 V vs. RHE (see Appendix I, Figure AI.3). This peak is most likely the stripping of CO from the electrode surface. After this stripping, the reduction peak is recovered and seen in all the subsequent scans that go up to 1.0 V vs. RHE. These observations suggest that adsorbed CO is

formed during the reduction peak in the first scan shown in Figure 4.5b, poisoning the electrode surface.

OLEMS analysis of the volatile products that were formed during CO_2 reduction on the Pd-Pt electrode showed mainly hydrogen (see Appendix I). However, the analysis of soluble products formed during CO_2 reduction on Pd-Pt showed the formation of formate / formic acid at very low overpotentials (see Figure 4.6). For both electrolytes, at pH 2 and pH 6.7, the onset potential for the reduction of CO_2 to formic acid was -0.15 V vs. RHE. This is a very significant

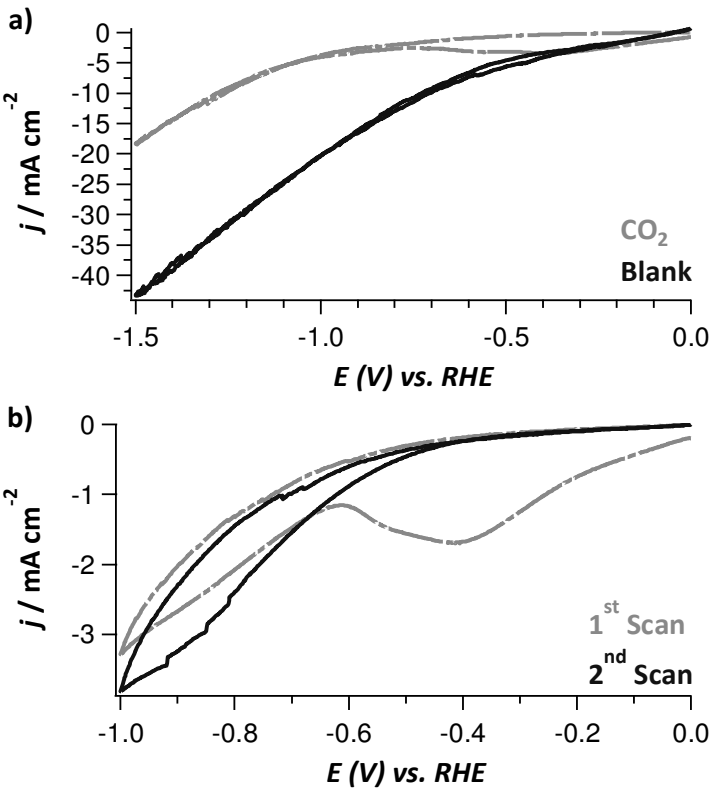

Figure 4.5 a) Cyclic voltammograms of a Pd-Pt electrode in a phosphate buffer at pH 6.7 (0.1 M KH_2PO_4 / 0.1 M K_2HPO_4) in the presence of argon (grey dash), and in the presence of CO_2 (black) at a scan rate of 50 mV/s, b) Cyclic voltammograms of a Pd-Pt electrode in a phosphate buffer at pH 6.7 (0.1 M KH_2PO_4 / 0.1 M K_2HPO_4) in the presence of CO_2 at a scan rate of 50 mV/s.

decrease compared with the onset potential of -1.2 V that was observed for the bulk palladium electrode at pH 6.7. The production of formate / formic acid in the pH 6.7 phosphate buffer shows a clear resemblance with the reduction peak observed in the voltammetry (Figure 4.5). This indicates that formate / formic acid Unfortunately, our system is not able to follow the production of CO in solution, since CO_2 also fragments into CO in the mass spectrometer. Some traces of methane and ethylene were observed at very negative potentials at both pH 2 and pH 6.7 as was also found with the bulk palladium electrode. Thus, the selectivity of the Pd-Pt electrode for volatile products did not change compared to bulk palladium.

is the main product formed during the reduction peak in the voltammetry. Remarkably, in a pH 2 electrolyte, the Pd-Pt electrode shows a continuous production of formic acid from -0.15 V, while in a pH 6.7 electrolyte formic acid production peaked in the low potential region (from -0.15 V to -0.7 V vs. RHE), whereas at potentials below -0.9 V vs. RHE the production of formic acid was seen to increase again (Figure 4.6b).

In comparison to recently reported catalysts for the reduction of CO_2 to formic acid our catalyst shows a considerably lower overpotential; a Sn/SnO_x reported by Chen et al.[19] started producing formic acid at -0.5 V vs. RHE and reached 40% faradaïc efficiency at -0.7 V vs. RHE with CO accounting for the remaining 60%, Zhang et al.[20] showed that the production of formic acid on SnO_2 nanocrystals on carbon black started at -1.0 V vs. SCE and reached a maximum of 86.2% faradaïc efficiency for formic acid at -1.8 V vs. SCE, and an homogeneous iridium pincer catalyst reported by Kang et al.[21] had an onset potential of approximately -1.0 V vs. NHE for the production of formic acid.

Since palladium is known to be able to reduce bicarbonate (HCO_3^-),[22] the ability of the Pd-Pt electrode to reduce bicarbonate was also tested. In this case, the phosphate buffer was replaced by a bicarbonate buffer solution and no CO_2 was purged through the electrolyte. The results of the reduction of bicarbonate shown in Figure 4.6c show a striking similarity to the reduction of CO_2 on the Pd-Pt electrode at pH 6.7 shown in Figure 4.6b. A low potential peak in the production of formic acid is seen, which agrees very well with the peak seen for

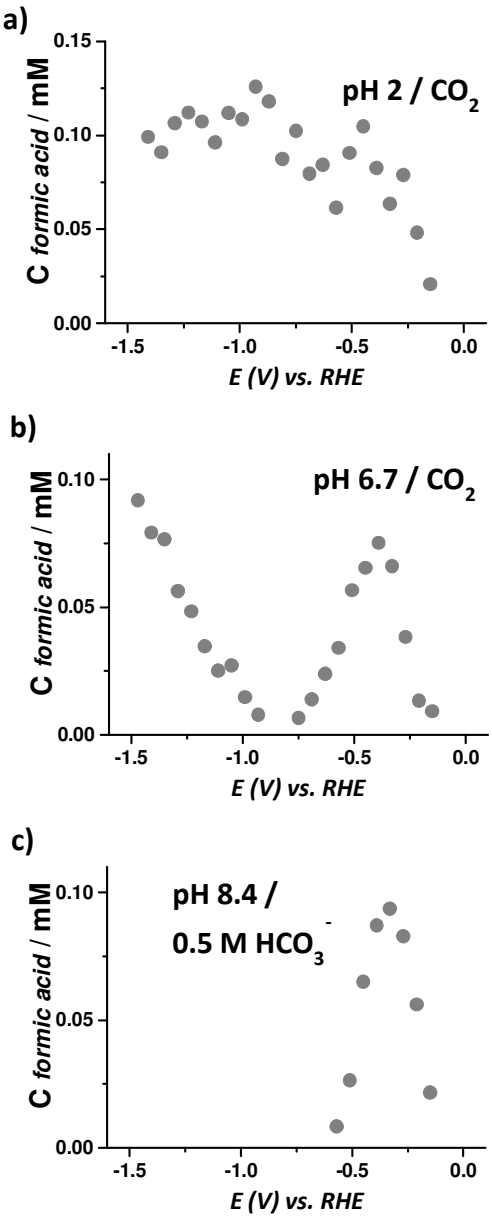

Figure 4.6 Formation of formic acid detected with online HPLC from a platinum electrode covered with palladium; **a)** formation of formic acid in a pH 2 phosphate buffer (0.1 M H_3PO_4/ 0.1 M KH_2PO_4) saturated with CO_2; **b)** formation of formic acid in a pH 6.7 phosphate buffer (0.1 M KH2PO4/ 0.1 M K_2HPO_4) saturated with CO_2; **c)** formation of formic acid in a 0.5 M $KHCO_3$ electrolyte without CO_2.

the production of formic acid from CO_2 at pH 6.7. This reduction peak must be due to either direct bicarbonate reduction or to the reduction of CO_2 generated from HCO_3^- due to the corresponding equilibrium between HCO_3^- and CO_2 near the electrode surface. At more negative potentials, the simultaneous HER leads to a local increase in pH near the electrode, converting HCO_3^- into CO_3^{2-} which cannot be reduced. This is supported by the observation that direct reduction of carbonate from a 0.5 M K_2CO_3 electrolyte did not yield any formate. Under CO_2 purging conditions (Figure 4.6b), CO_2 is still reduced at these potentials either because CO_2 conversion into HCO_3^-/CO_3^{2-} is slow or because the solution is locally saturated with HCO_3^-/CO_3^{2-}.

The different catalytic properties of Pd-Pt compared to Pd can be due to an electronic or geometric effect that the platinum substrate has on the palladium layers covering it. It is known that Pd-Pt slows down CO poisoning during formic acid oxidation.[17] In addition, we believe that an additional important effect of the thin-layer palladium is to suppress hydrogen absorption (in comparison with bulk palladium), and this may have an effect on its reduction properties.

Finally, we show that the formic acid oxidation and CO_2 reduction can occur reversibly on the Pd-Pt electrode, similar to formate dehydrogenase enzymes (FDH). The results are shown in Figure 4.7. To avoid oscillations in the formic acid oxidation part of the cyclic voltammogram the concentration of the phosphate buffer in the electrolyte was raised.[17] Figure 4.7a shows that formic acid oxidation (between 0.2 V to 1.0 V vs. RHE) and CO_2 reduction (between -0.05 V to -0.35 V vs. RHE) are observed when both formate and CO_2 are present in a pH 6.7 phosphate buffer electrolyte. Notice again that the peak potential of CO_2 reduction coincides with the peak in production of formic acid seen earlier in Figure 4.6b. Figure 4.7c and 4.7d show the detection of CO_2 in the positive potential range and the formation of formic acid in the negative potential range respectively. This is thus a clear indication that this catalyst is able to perform both CO_2 reduction and formic acid oxidation. When the electrolyte was not purged with CO_2, the peak related to CO_2 reduction was only seen after the oxidation of formic acid. This indicates that the CO_2 that was formed from formic acid oxidation was reduced back to formic acid.

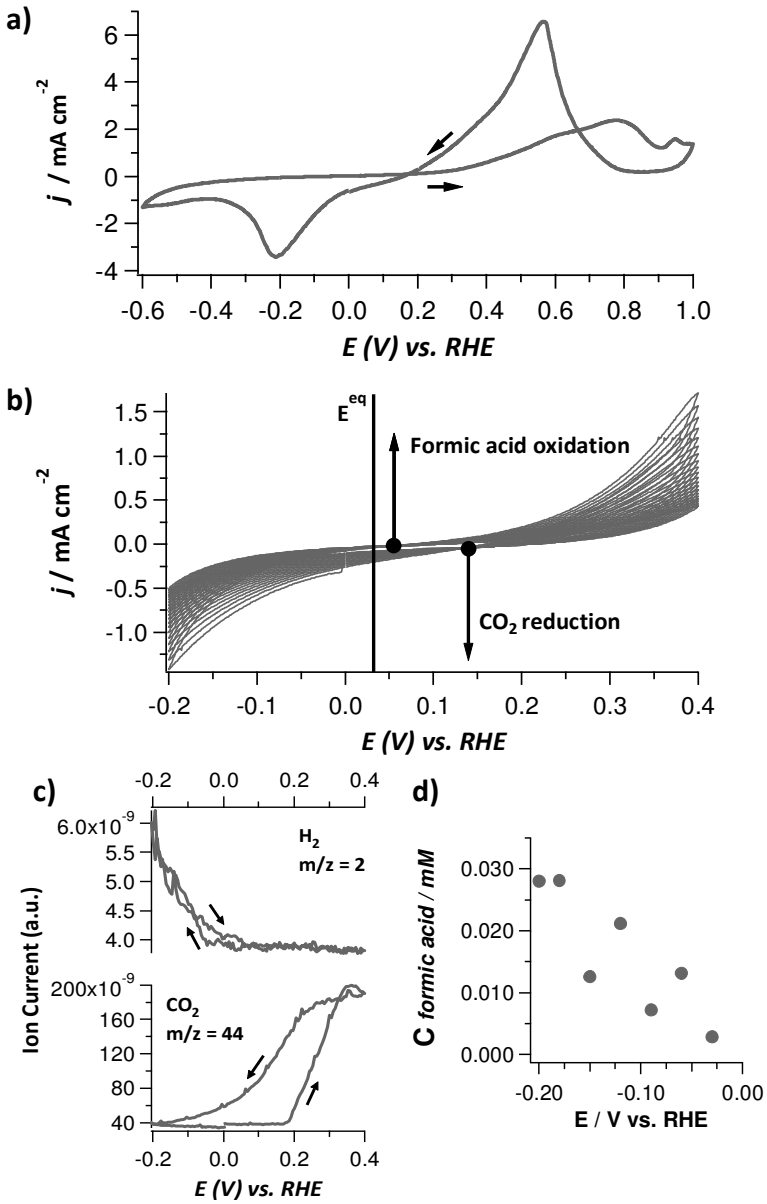

Figure 4.7 a) Cyclic voltammogram of formic acid oxidation and CO_2 reduction in a pH 6.7 phosphate buffer (0.2 M NaH_2PO_4/ 0.2 M Na_2HPO_4) with 25 mM NaHCOO on a Pd-Pt electrode at a scan rate of 50 mV/s in the presence of CO_2, **b)** 20 consecutive cyclic voltammograms at 50 mV/s of formic acid oxidation and CO_2 reduction in the same electrolyte in the reversibility region, **c)** Formation of CO_2 and H_2 as detected with OLEMS, **d)** Formation of formic acid as detected with online HPLC.

To demonstrate reversible interconversion between carbon dioxide and formate / formic acid, 20 consecutive cyclic voltammograms were made in the region around the equilibrium potential (-0.2 V to 0.4 V vs. RHE) (Figure 4.7b). Although the reversibility shown in Figure 4.7b is certainly not as perfect as for the H_2/H^+ couple on platinum, it is comparable to the voltammetry for the $CO_2/HCOO^-$ couple on FDH shown by Reda et al..[23] The activity decreases during these 20 voltammograms, again indicating that the catalyst is poisoned by adsorbed CO formed in the potential window around the reversible potential. Also note that there is simultaneous evolution of hydrogen during CO_2 reduction.

4.4 Conclusions

In conclusion, in this Chapter we demonstrated the reversible catalyst principle, namely that catalysts that are active for the oxidation of formic acid should also be active for the reduction of CO_2 to formic acid. Such a catalyst was developed by electrodepositing palladium on a polycrystalline platinum substrate. This catalyst is able to reduce CO_2 to formic acid starting from -0.05 V vs. RHE at pH 6.7, compared to an onset potential for the reduction of CO2 to formic acid of -1.2 V vs. RHE for a bare palladium electrode at the same pH. The Pd-Pt electrode is also able to reduce bicarbonate as well as to reversibly convert CO_2 into formic acid and vice versa. The main challenge in the further development of such a "reversible" metallic catalyst for CO_2 reduction is to avoid CO poisoning and to suppress concomitant H_2 evolution.

References

(1) Gattrell, M.; Gupta, N.; Co, A. *Energy Convers. Manage.* **2007**, *48*, 1255-1265.

(2) Whipple, D.T.K.; Kenis, P.J.A.; *J. Phys. Chem. Lett.* **2010**, *1*, 3451-3458.

(3) Y. Hori in *Modern Aspects of Electrochemistry*, Vol. 42 (Eds: C.G. Vayenas, R.E. White, M.E. Gamboa-Aldeco), Springer, New York, 2008, pp. 89-189.

(4) Chaplin, R.P.S.; Wragg, A.A. *J. Appl. Electrochem.* **2003**, *33*, 1107-1123.

(5) Yu, X.; Pickup, P.G.; *J. Power Sources* **2008**, *182*, 124-132.

(6) Jitaru, M.; Lowy, D.A.; Toma, M.; Toma, B.C.; Oniciu, L. *J. Appl. Electrochem.* **1997**, *27*, 875-889.

(7) Zhang, S.; Kang, P.; Meyer, T.J. *J. Am. Chem. Soc.* **2014**, *136*, 1734-1737.

(8) Armstrong, F.A.; Hirst, J.; *PNAS* **2011**, *108*, 14049-14054.

(9) M.T.M. Koper *J. Electroanal. Chem.* **2011**, *660*, 254-260.

(10) Yu, X.; Pickup, P.G. *J. Appl. Electrochem.* **2011**, *41*, 589-597.

(11) Hoshi, N.; Hori, Y.; *Electrochim. Acta* **2000**, *45*, 4263-4270.

(12) Sánchez- Sánchez, C. M.; Souza-Garcia, J.; Herrero, E.; Aldaz, A. *J. Electroanal. Chem.* **2012**, *668*, 51-59.

(13) Wonders, A.H.; Housmans, T.H.M.; Rosca, V.; Koper, M.T.M. *J. Appl. Electrochem.* **2006**, *36*, 1215-1221.

(14) Kwon, Y.; Koper, M.T.M.; Anal. Chem. **2010**, *82*, 5420-5424.

(15) Ohkawa, K.; Hashimoto, K.; Fujishima, A. *J. Electroanal. Chem.* **1993**, *345*, 445-456.

(16) Hori, Y.; Wakabe H.; Tsukamoto, T.; Koga, O. *Electrochim. Acta* **1994**, *39*, 1833-1839.

(17) Baldauf, M.; Kolb, D.M. *J. Phys. Chem.* **1996**, *100*, 11375-11381.

(18) Grdeń, M.; Paruszewska, A.; Czerwiński, A. *J. Electroanal. Chem.* **2001**, *502*, 91-99

(19) Chen, Y.; Kanan, M.W. *J. Am. Chem. Soc.* **2012**, *134*, 1986-1989

(20) Zhang, S.; Kang, P.; Meyer, T.J. *J. Am. Chem. Soc.* **2014**, *136*, 1734-1737

(21) P. Kang, S. Zhang, T.J. Meyer, M. Brookhart, Angew. Chem. Int. Ed. 53 (2014) 1-6

(22) Spichiger-Ulmann, M.; Augustynski, J.; *J. Chem. Soc., Faraday Trans.* **1985**, *81*, 713-716.

(23) Reda, T.; Plugge, C.M.; Abram, N.J.; Hirst, J. *PNAS* **2008**, *105*, 10654-10658.